Atmos. Meas. Tech. Discuss., 7, 1059–1073, 2014
www.atmos-meas-tech-discuss.net/7/1059/2014/
doi:10.5194/amtd-7-1059-2014

Atmospheric Measurement Techniques Discussions

Airborne multiwavelength High Spectral Resolution Lidar (HSRL-2) observations during TCAP 2012: vertical profiles of optical and microphysical properties of a smoke/urban haze plume over the northeastern coast of the US

D. Müller[1,2], C. A. Hostetler[3], R. A. Ferrare[3], S. P. Burton[3], E. Chemyakin[2], A. Kolgotin[4], J. W. Hair[3], A. L. Cook[3], D. B. Harper[3], R. R. Rogers[3], R. W. Hare[3], C. S. Cleckner[3], M. D. Obland[3], J. Tomlinson[5], L. K. Berg[5], and B. Schmid[5]

[1]University of Hertfordshire, Hatfield, Hertfordshire, UK
[2]Science Systems and Applications, Inc., NASA Langley Research Center, Hampton, VA, USA
[3]NASA Langley Research Center, Hampton, VA, USA
[4]Physics Instrumentation Center, Troitsk, Russia
[5]Pacific Northwest National Laboratory, Richland, WA, USA

Received: 14 January 2014 – Accepted: 27 January 2014 – Published: 6 February 2014

Correspondence to: D. Müller (d.mueller@herts.ac.uk)

Published by Copernicus Publications on behalf of the European Geosciences Union.

Abstract

We present measurements acquired by the world's first airborne multiwavelength High Spectral Resolution Lidar (HSRL-2), developed by NASA Langley Research Center. The instrument was operated during Phase 1 of the Department of Energy (DOE) Two-Column Aerosol Project (TCAP)in July 2012. We observed pollution outflow from the northeast coast of the US out over the West Atlantic Ocean. Lidar ratios were 50–60 sr at 355 nm and 60–70 sr at 532 nm. Extinction-related Ångström exponents were on average 1.2–1.7 indicating comparably small particles. Our novel automated, unsupervised data inversion algorithm retrieves particle effective radii of approximately 0.2 µm, which is in agreement with the large Ångström exponents. We find good agreement with particle size parameters obtained from coincident in situ measurements carried out with the DOE Gulfstream-1 aircraft.

1 Introduction

The world's first airborne "3 backscatter (β) + 2 extinction (α)" multiwavelength High Spectral Resolution Lidar (HSRL-2) acquired data during the first Intensive Observation Period (7–30 July 2012) of the Department of Energy (DOE) Two-Column Aerosol Project (TCAP). TCAP goals included quantifying aerosol properties and radiation and cloud characteristics at a location subject to both clear and cloudy conditions, and both clean and polluted conditions.

HSRL-2 is the successor of HSRL-1 which has been operating in various field campaigns since 2006 (Hair et al., 2008). Like HSRL-1, HSRL-2 measures backscatter, extinction, and depolarization at 532 nm and backscatter and depolarization at 1064 nm. In addition, HSRL-2 also measures extinction, backscattering, and depolarization at 355 nm.

We present the first results of HSRL-2 "$3\beta + 2\alpha$" measurements of pollution that was transported from the US and Canada out over the western Atlantic Ocean during TCAP.

AMTD
7, 1059–1073, 2014

This is the first use of our prototype software that delivers profiles of particle microphysical parameters in near-real time from the inversion of the optical profiles measured by HSRL-2 aboard the NASA B-200 King Air aircraft. We show a comparison of our results to coincident in situ measurements of particle size parameters acquired by the DOE Gulfstream-1 (G-1) aircraft. Section 2 summarizes the methodologies. Section 3 presents a measurement example. Section 4 closes with a summary and an outlook.

2 Methodology

HSRL-2 operates at laser wavelengths of 355, 532, and 1064 nm. The basic HSRL technique is described by Eloranta (2005). The new feature of HSRL-2 compared to HSRL-1 is that it measures the particle volume extinction coefficient not only at 532 nm but also at 355 nm. For this purpose novel hardware based on Michelson interferometry has been developed. An iodine-vapor filter is used for the extinction-coefficient measurements at 532 nm. Details on the instrument, the novel channel at 355 nm, and data analysis procedures will be given in a separate publication.

HSRL-2 measures profiles of particle backscatter coefficients and linear particle depolarization ratios at 355, 532, and 1064, and particle volume extinction coefficients at 355 and 532 nm. The uncertainties of the data are governed by various factors, like hardware and its calibration, signal calibration, signal-to-noise ratio, and signal averaging in time and space. The data were temporally and spatially averaged to make the random error insignificant, so that we could focus in this first test on the retrievals and comparisons of the inversion software. We obtained uncertainties of 0.1–3 % of the optical data, depending on the measurement channels. These values are more than adequate for the requirement set out for trustworthy microphysical retrievals nearly 10 yr ago (Ansmann and Müller, 2005). HSRL-2 is well capable of delivering optical data with considerably better temporal resolution for space-borne applications. One of the next steps in our inversion algorithm development is to meet the standards of these high-resolution measurements such that the data inversion products stay within

AMTD
7, 1059–1073, 2014

the retrieval uncertainties we currently achieve for the 5 min averages of the optical profiles.

From the measured optical data we calculate profiles of extinction- and backscatter-related Ångström exponents and the lidar ratios at 355 and 532 nm which allows for detailed aerosol typing; see Burton et al. (2012) for examples of aerosol typing with HSRL-1 data. Measuring backscatter coefficients at 355, 532, and 1064 nm and extinction coefficients at 355 and 532 nm is the minimum requirement for applying data inversion methods (Ansmann and Müller, 2005) that allow us to derive particle size distributions which are used to compute effective radius, number, surface-area, and volume concentrations. The solution space of the complex refractive indices implicitly follows from the solution space defined by the size parameters. Before the commissioning of HSRL-2 these inversion methods were only used for the analysis of ground-based multiwavelength Raman lidar systems which are mainly operated by EARLINET (Bösenberg et al., 2003).

HSRL-2 has advantages over ground-based multiwavelength Raman lidars: the temporal resolution of the optical profiles is significantly higher due to the higher signal-to-noise ratios and daytime measurement is no problem for HSRL-2, whereas this capability still is not possible on a routine basis with multiwavelength Raman lidar. Raman lidars are stationary and the ground-based systems suffer from data loss near the ground due to the incomplete overlap between outgoing laser beam and receiver field of view of the detector system.

HSRL-2 is the motivation for developing the next generation of inversion methodology that allows us to process a high volume of data in an unsupervised, automated manner in real time with significantly enhanced accuracy of the inversion data products. We want to prepare the software for application with a space-borne version of the multiwavelength HSRL. The procedures applied to identify the solution space are still based on the established methods described by Ansmann and Müller (2005). Simulation results show that we can infer particle effective radius, number, surface-area and volume concentration to accuracy levels that are at least as good as the ones we

AMTD
7, 1059–1073, 2014

obtain with the manually operated version of the software (Ansmann and Müller, 2005). Improvements of the procedures that are used to identify the solution space now allow us to derive number concentration to an accuracy of approximately 50–100 %. Details on this automated software and the results of the simulations studies will be given in future contributions.

We compare our data products to in situ data of particle size distributions measured aboard the DOE G-1 aircraft. The particle size distributions (PSD) are comprised of measurements made with the Ultra-High Sensitivity Aerosol Spectrometer – Airborne (UHSAS-A), Passive Cavity Aerosol Spectrometer (PCASP), and the Cloud Aerosol Spectrometer (CAS). The data are subsequently corrected for transmission efficiency and mapped through the use of a weighted average to a 34-bin distribution starting at a radius of 50 nm and ending at a radius of 5.35 µm. This size range was selected to closely match the HSRL data inversion radius range. The aerosol probes were calibrated throughout the TCAP field campaign using PSL beads. For the super-micron sizes measured by the CAS glass beads were used. Any cloud contaminated data were flagged and subsequently not used. All PSDs were measured at close to ambient conditions. The PCASP and UHSAS-A anti-ice heaters were not operated during the campaign. The CAS is an open path instrument. Therefore, no corrections for relative humidity were attempted.

3 Results and discussion

The first phase of TCAP was characterized by outflow of pollution out over the western Atlantic Ocean. Smoke from fires that occurred in Canada may have episodically contributed to this outflow. HSRL-2 acquired data on 11 days between 7 July and 30 July 2012, which includes the transit flights between NASA Langley Research Center, VA, and Barnstable Airport (41.67° N, 70.29° W), MA. The B-200 flew approximately 3–3.5 h during each of the research flights. In this contribution we focus on the measurements carried out on 17, 22 and 25 July 2012.

AMTD
7, 1059–1073, 2014

Optical depths measured with AERONET Sun photometer at Barnstable Airport varied between 0.06–0.6 (at 500 nm); level 2.0 data. Maximum daily-mean optical depth was 0.459 on 18 July and 0.331 on 17 July 2012. Another AERONET Sun photometer was operated at a coastal station at 41.3° N, 70.55° W. Optical depth varied between 0.046–0.5 (at 500 nm). Daily-mean optical depth was 0.386 on 18 July and 0.243 on 17 July 2012; level 1.5 data.

The mean height of the pollution layers did not exceed 4 km a.s.l. with few exceptions in some portions of the flight tracks. The G-1 flew inside the pollution layers at various flight levels, and also carried out spirals from near sea level to the top of the pollution layers on several occasions. The B-200 flew at 8–9 km a.s.l. and thus always stayed above the pollution layers. For our comparison we selected only those flight segments during which the G-1 carried out spirals during or shortly after overflights by the B-200 aircraft. The maximum allowed distance from the HSRL profile to the approximate center of the spiral was 35 km. The time difference to the beginning or end of the spiral of the G-1 was at most 22 min. The spiral took about 11–12 min to complete and covered about 8 km on 17 July. In this way we obtain the best possible data from the G-1 for our comparison study.

Figure 1 shows the example of the HSRL-2 measurement on 17 July 2012. Most of the aerosol particles were below 3 km a.s.l. A plume reaching heights up to 5 km was encountered during a short segment of the flight. Extinction coefficients remained comparably stable throughout the flight. Optical depth over the ocean generally varied between 0.3–0.45 at 355 nm and 0.2–0.25 at 532 nm on 17 July 2012.

The extinction-related Ångström exponent was on average 1.2–1.7. The patch-like structure shown in Fig. 1d shows an inhomogeneous structure with values varying between 1 and 2.5. The lidar ratios at 355 and 532 nm varied on average between 50–70 sr in the pollution layers. The lidar ratio at 355 nm was similar or slightly lower to the one at 532 nm. There was no significant decrease of the Ångström exponent and the lidar ratios near the ocean surface which would indicate that marine particles significantly contributed to the aerosol load in the marine boundary layer.

AMTD
7, 1059–1073, 2014

HYSPLIT backtrajectories show that on 17 July 2012 the airflow was from the Great Lakes to the Atlantic Ocean. Satellite images point at the presence of smoke particles. The age of the smoke likely was less than 48 h. We assume that the smoke mixed with the urban haze over the northeastern US before it was transported out over the North Atlantic.

We selected the measurement around 16:00 UTC. We averaged the individual optical profiles in this 5 min time-segment, and we split the profiles into height layers of 150 m geometrical depth. We obtained 20 sets of $3\beta + 2\alpha$ coefficients, which then were processed with our automated algorithm. The data processing including error analysis for these 20 data points took approximately 6 min. We generated nearly 11.5 million individual solutions from which 2000 solutions were accepted according to the mathematical and physical constraints used in our algorithm. We then produced the profiles of the microphysical particle parameters from these 2000 solutions.

Figure 2 shows that effective radius does not significantly vary with height. It is approximately 0.2 µm which is characteristic for urban aerosols and/or smoke, e.g. Müller et al. (2007) and references therein. The inversion results agree within error bars with the in situ measurements. The sampling volume of the in situ probe is significantly smaller than the sampling volume of the lidar. Small scale variations of particle effective radius cannot be resolved with our inversion methodology. Number, surface-area and volume-concentration obtained from data inversion and in situ measurements are close to each other.

In general the size range within which in situ instruments collect particles is different from the size range used in the data inversion An example of how changing the lower radius limit can alter particle size parameters is given in Table 1 of Wandinger et al. (2002). This effect of variable lower and upper limit must be considered in any kind of study that compares data from remote sensing instruments, which use data inversion methods, to data from in situ probes. In our study we compare approximately the same lower radius range, i.e., inversion results use as lower limit approximately 54 nm and the in situ measurements start measuring at approximately 50 nm radius. With regard

AMTD
7, 1059–1073, 2014

to the upper threshold we used approximately 6 µm radius for the inversion and 5.35 µm radius for the in situ data.

Figure 3 shows the correlation of (a) the Ångström exponent measured with HSRL-2 vs. effective radius determined with the inversion algorithm and with the in situ instruments, respectively. Also shown are the correlation of (b) effective radius, (c) number, (d) surface-area, and (e) volume concentration obtained from the lidar-data inversion and the in situ measurements. We averaged the in situ data across 150 m height intervals for this comparison; 17–56 data points were averaged in each of the height bins. The plots also show the results for the measurements on 22 and 25 July 2012; on these two days spiral flights of the G-1 were done. The number of data points that can be used for the comparison is significantly smaller on these two days.

The correlation shown in Fig. 3a is high for effective radius obtained with our inversion algorithm. The correlation of effective radius from the in situ measurements shows a larger scatter, which has to be expected as we compare data products from two different methods, i.e. Ångström exponents from HSRL-2 and particle size from in situ measurements. Several reasons can be the cause for the weaker correlation, e.g. (1) there is no perfect collocation in measurements space and time of the two instruments; (2) in situ instruments dry the particles off before a humidity correction is applied, even though a humidity correction did not seem necessary in the present case; (3) the in situ measurements were taken with considerably higher vertical resolution (spirals) than the Ångström exponents measured with HSRL-2, and subsequently averaged to the vertical resolution of the HSRL-2 measurements; (4) the atmospheric volume observed by the lidar is considerably larger than the measurement volume of the in situ instruments, and thus averaging effects of the observed air volume may play a role, too. The weaker correlation between effective radius measured with the in situ instruments and the Ångström exponents measured with HSRL-2 may also explain the weaker correlation of the data products shown in Fig. 3b–e.

Mean values of effective radius from data inversion are on average lower than effective radius from the in situ measurements, see Fig. 3b. The same holds true for

AMTD
7, 1059–1073, 2014

number concentration. We find the opposite behavior for surface-area and volume concentration. In view of the fact that this is the first test of our automated software with experimental data and in view of the various error sources involved in both methods we consider this comparison satisfactory. A more detailed comparison study that will include data from TCAP and two more field campaigns that took place in 2013 will be presented in a future contribution.

Figure 3 shows the mean values of the data products. We computed uncertainty bars for the 47 data points available from both methods (150 m height intervals). Uncertainties of number concentration are 34 % ± 15 % and 30 % ± 13 % from in situ and from data inversion, respectively. Uncertainties of surface-area concentration are 39 % ± 17 % and 14 % ± 7 % from in situ and data inversion. Uncertainties of volume concentration are 52 % ± 20 % and 21 % ± 7 %. Effective radius shows uncertainties of 38 % ± 15 % and 12 % ± 2 %. This is a very simplified presentation of the uncertainties from both methods. We have only few data points available, the errors distribution is not Gauss-distributed, and there are some outliers. Details of error analysis will be given in a more extended version of this paper.

4 Conclusions

We presented first results of aerosol measurements with NASA Langley Research Center's High Spectral Resolution Lidar, HSRL-2. We used HSRL-2 data to test the performance of our newly developed automated, unsupervised inversion algorithm with experimental data for the first time. HSRL-2 and the inversion software will be used to investigate the possibility of operating a 3 backscatter + 2 extinction HSRL in space. Such an instrument could be part of NASA's ACE (Aerosol-Clouds-Ecosystems) mission.

Particle effective radius and Ångström exponents are in agreement with literature values of urban haze and/or biomass-burning smoke. We find satisfactory correlation

AMTD
7, 1059–1073, 2014

of our data products to in situ measurements of particle size distributions measured aboard the DOE G-1 aircraft.

The lidar microphysical retrievals are not as detailed as those made in situ on the G-1 aircraft. The *curtains* of horizontally and vertically resolved microphysical information enable characterization of the aerosol properties above and below the G-1 flight altitude, and hence characterization of the entire column. In particular, the lidar curtains of these aerosol properties will be important for TCAP radiative closure studies. More generally, applications of the HSRL-2 data set include studies of aerosol direct and indirect effects, investigations of aerosol–cloud interactions, assessment of chemical transport models, and air quality studies.

We continue to investigate the quality of our inversion data products. Additional data are available from the DISCOVER-AQ campaigns that took place in California in January–February 2013 and in Texas in September 2013. We will further improve the quality of other data products like the imaginary part of the complex refractive index that allows us to compute profiles of the absorption coefficient and the single-scattering albedo. We will study the accuracy of retrieving these optical parameters as wavelength-dependent quantities. We recently started to investigate the benefit of using combinations of data from different instruments, e.g. HSRL-2 and passive space-borne sensors that could be part of the ACE mission.

Acknowledgements. The authors thank the NASA Langley B-200 King Air flight crew for their outstanding work supporting research flights. Support for the HSRL-2 and RSP flight operations on TCAP was provided by the DOE ARM program: Interagency Agreement DE-SC0006730. Support for data analysis was provided in part by the DOE Atmospheric System Research (ASR) program. Support for the development of HSRL-2 was provided by the NASA Science Mission Directorate, ESTO, AITT, and Radiation Science Program. We thank C. Flynn, R. Wagener, L. Gregory, and P. Russell at the Barnstable AERONET station for providing data. The AERONET data at MVCO are provided by H. Feng and H. M. Sosik.

AMTD
7, 1059–1073, 2014

References

Ansmann, A. and Müller, D.: Lidar and atmospheric aerosol particles, in: Lidar, Range-Resolved Optical Remote Sensing of the Atmosphere, edited by: Weitkamp, C., Springer, New York, 105–141, 2005. 1062, 1063, 1064

Burton, S. P., Ferrare, R. A., Hostetler, C. A., Hair, J. W., Rogers, R. R., Obland, M. D., Butler, C. F., Cook, A. L., Harper, D. B., and Froyd, K. D.: Aerosol classification using airborne High Spectral Resolution Lidar measurements – methodology and examples, Atmos. Meas. Tech., 5, 73–98, doi:10.5194/amt-5-73-2012, 2012. 1063

Eloranta, E. W.: High spectral resolution lidar, in: Lidar, Range-Resolved Optical Remote Sensing of the Atmosphere, edited by: Weitkamp, C., Springer, New York, 143–163, 2005. 1062

Bösenberg, J., Matthias, V., Amodeo, A., et al.: EARLINET: a European Aerosol Research Lidar Network to establish an aerosol climatology, Max Planck Institute for Meteorology, Report No. 348, 155–158, 2003. 1063

Hair, J. W., Hostetler, C. A., Cook, A. L., Harper, D. B., Ferrare, R. A., Mack, T. L., Welch, W., Izquierdo, L. R., and Hovis, F. E.: Airborne high-spectral-resolution lidar for profiling aerosol optical profiles, Appl. Optics, 47, 6734–6752, doi:10.1364/AO.47.006734, 2008. 1061

Müller, D., Mattis, I., Ansmann, A., Wandinger, U., Ritter, C., and Kaiser, D.: Multiwavelength Raman lidar observations of particle growth during long-range transport of forest-fire smoke in the free troposphere, Geophys. Res. Letts., 34, L05803, doi:10.1029/2006GL027936, 2007. 1066

Wandinger, U., Müller, D., Böckmann, C., Althausen, D., Matthias, V., Bösenberg, J., Weiss, V., Fiebig, M., Wendisch, M., Stohl, A., and Ansmann, A.: Optical and microphysical characterization of biomass-burning and industrial-pollution aerosols from multiwavelength lidar and aircraft measurements, J. Geophys. Res., 107, 8125, doi:10.1029/2000JD000202, 2002. 1066

AMTD
7, 1059–1073, 2014

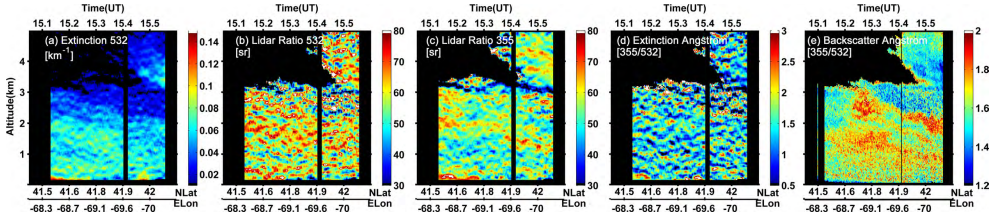

Fig. 1. Curtain plot of the HSRL-2 measurement on 12 July 2012, 14:20–17:20 UTC. Shown are the mean values of the profiles of **(a)** the extinction coefficient at 532, the lidar ratios at **(b)** 532 and **(c)** 355 nm, **(d)** the extinction-related and **(e)** the backscatter-related Ångström exponent at 355/532 nm. Each profile is based on a 10 s signal-sampling rate. The vertical resolution is 150 m. The position of the aircraft during the flight is shown on the *x* axis.

AMTD
7, 1059–1073, 2014

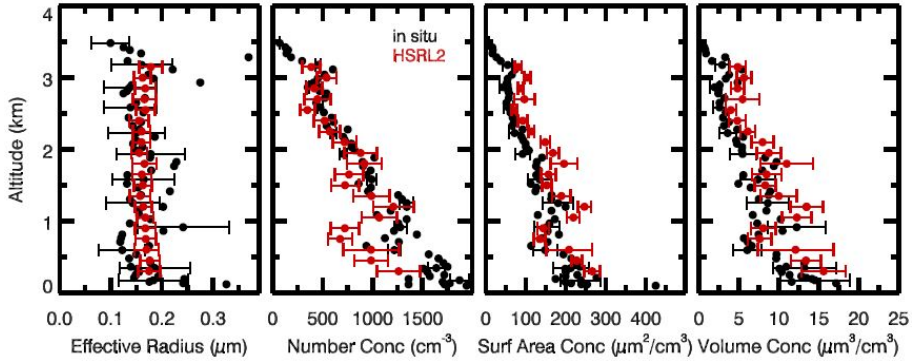

Fig. 2. Microphysical parameters retrieved from the inversion method (red) and from the G-1 in situ measurements (black) on 17 July 2012. The measurement time was 16:00–16:05 UTC for the inversion results and from 15:45–15:56 UTC for the in situ data. The lidar measurements were obtained 2 km from the approximate G-1 spiral center. The inversion results represent height intervals of 150 m. The in situ data were taken with considerably higher spatial resolution. Error bars of the individual in situ data points are composed of two types, counting and sizing. The error bars denote one-standard deviation. Details on the error computations will be given in a separate publication.

AMTD
7, 1059–1073, 2014

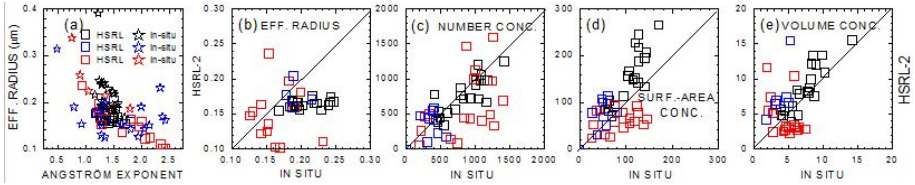

Fig. 3. (a) Correlation of Ångström exponents measured with HSRL-2 vs. effective radius (in μm) obtained from data inversion (boxes) and vs. effective radius from in situ (open stars). Correlation between inversion results and in situ results for **(b)** effective radius, **(c)** number concentration (cm^{-1}), **(d)** surface-area concentration ($\mu m^2\,cm^{-3}$), and **(e)** volume concentration ($\mu m^3\,cm^{-3}$) on 17 July (black), 22 July (red), and 25 July (blue).

AMTD
7, 1059–1073, 2014